

3D Printing And Free-form Surface Coating Based on 6-DOF Robot

Huixiong Zeng*, Mingqi Feng*, Jiafu Zhuang*, Rongsheng Cai[†], Yinhui Xie*, Jun Li*

*Quanzhou Institute of Equipment Manufacturing, Chinese Academy of Science, Quanzhou, China

[†]Quanzhou College of Technology, Quanzhou, China

Abstract—At present, most of the 3D printing facilities are 3 degrees of freedom (DOF) that formed by planar stacking, which cannot achieve free-form surface spraying or other high DOF required operations. However, in a way, this problem can be solved by using a 6-axis manipulator, which is the future development trend of the 3D printing facilities. In this paper, a UR manipulator is used to realize the 3D printing function, especially the coating procedure of biomaterials, such as coating hydroxyapatite on the surface of artificial models. By dismantling the steps of our methodology, we firstly obtain the point cloud data of the 3D models and reconstruct the point cloud with a straightforward algorithm for the further subsequent path planning of UR manipulator for 3D printing. After that, the control parameter calculation of the printing path of UR is explained in detail. Finally, the printing accuracy of UR and interlayer uniformity of the 3D model are optimized by iterating the related experiments. The high-quality printed samples of the 3D models prove that our research has successfully achieved the practical application of UR manipulator in 3D printing.

Index Terms—3D-printing, Robot, Free-form surface, Reconstruction, Path planning

I. INTRODUCTION

3D printing is a kind of rapid prototyping technology. Based on digital model files, it uses powdered metals or plastics and other adhesive materials to build objects by layer-by-layer printing[1]. 3D bio-printing is mainly based on Computer-aided Additive Manufacturing (CAM) technology, which accurately controls the position, combination, or interaction of biological materials, biological cells, and growth factors in the overall 3D structure to make them biologically active. At present, bio-manufacturing is the most cutting-edge field of 3D printing. The three-dimensional controlled assembly of cells directly allows humans to control the 3D assembly of individual cells and cell clusters in accordance with the digital model of organ anatomy, eventually achieving integration into the human metabolic system for the repair and replacement of damaged tissues and organs[2-3].

The traditional 3D printing is the process of additive forming, that is, by stacking model slices layer by layer,

*This work was supported by the National Key Research and Development Program of China (No. 2016YFC11000501) and Laboratory of Robotics and Intelligent Systems (CAS, Quanzhou).

Huixiong Zeng, Mingqi Feng, Jiafu Zhuang, Yinhui Xie, Jun Li* (corresponding author)* are with Quanzhou Institute of Equipment Manufacturing, Chinese Academy of Sciences, Quanzhou, China. Rongsheng Cai is with Quanzhou College of Technology, Quanzhou, China. (zenghx@fjirsm.ac.cn, mqfeng111@163.com, jiafuzhuang@fjirsm.ac.cn, xyh1932@fjirsm.ac.cn, junli@fjirsm.ac.cn, 125066774@qq.com).

each layer can only perform plane motion. And the attitude of the print nozzle can not be adjusted, so the processing freedom is low. Besides, the step effect is easy to occur, and operations such as printing of spatial free-form surfaces are not competent[4-5]. With the development of 3D bio-printing and the popularization of applications, the construction of human organs such as bones, liver and skin have been realized by special 3D printer [6-8]. Due to the complicated construction of the organ of human body, operations such as surface coating require high DOF, so the planar printing method is difficult to meet the requirements of 3D bio-printing in the future. With the wide application of robotics technology, more and more robots applied to the scenes which required high DOF such as spraying and polishing [9-12], its performance fully meets the development trend of 3D printing.

At present, a number of robot-assisted additive manufacturing processes have been presented in the literature [13-17]. Wang et al. [13] utilized point cloud slicing for a spray painting robot, and Kim et al. [14] split CAD models into distinct parts for cooperative tool path planning. Wang et al. [15] used an adaptive compensation algorithm for printing letters on a curved B-spline surface. Barnett et al. [16] introduced a large-scale 3D printer, which used a six-degree-of-freedom cable-suspended robot for positioning. Chengkai et al. [17] presents a new method to fabricate 3D models on a robotic printing system, and materials are accumulated inside the volume along curved tool-paths so that the need of supporting structures can be tremendously reduced.

To summarize, the key to using robots for 3D printing is the planning of the print path, which depends on the data processing of the 3D model. At present there are two main methods for robot tool trajectory planning based on 3D model: One is the slicing intersection method based on discrete point features such as stl or point cloud to obtain the robot tool trajectory; the other is obtained the tool processing code through UG and other CAM software, and then calculate the robot tool trajectory. The existing methods have a large computational complexity for 3D model reconstruction, and the algorithm is complex.

Our method has simple processing, high versatility and high precision for the 3D model reconstruction, which provides great convenience for the subsequent robot trajectory planning. This study is aim to achieve 3D printing of biomaterials using hydroxyapatite as a material, especially for the coating of hydroxyapatite on free-form surface models. We use the line

laser sensor to acquire the point cloud data on the surface of the 3D model. Then the printed path trajectory and control parameters of the manipulator are obtained by processing the point cloud. And we improved the control parameters through experiments to optimize the printing results. The following chapters of this paper are as follows: Section II introduces the control system framework; Section III explains how to optimize the printing accuracy and plane uniformity through the experiment of traditional plane printing; Section IV details the data processing process of surface coating by manipulator; Section V shows the results of the printing experiment.

II. OVERVIEW OF CONTROL SYSTEM

The 3D printing system based on robot is shown in the Fig. 1, the printing manipulator is a UR3 robot with a needle tube at the end, and inkjet printing is realized by pressing the material in the needle tube. The printed material is located on a four-axis platform. The movable platform is used for coordinate calibration of UR3 and the model. Meanwhile, we monitor the position of the end point of the needle and observe the jitter and pause of UR3 during printing, so that we can optimize the control parameters such as speed and the delay time of commands.

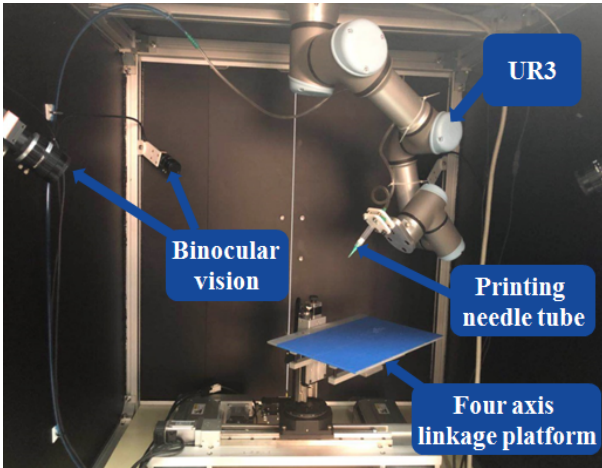


Fig. 1. Overview of 3D printing system

According to different 3D printing requirements, the print model preprocessing is divided into two different processes, as shown in Fig. 2. For planar additive forming 3D printing, the processing flow of the model is to plan path after slicing, and then integrated to form a complete planning path. For the free-form surface coating, the processing flow is first to convert the surface into a point cloud model with a certain interval, and then triangulated to obtain the normal vector of each point. Secondly, the attitude parameters of UR3 are calculated according to the normal vector. Finally, the point cloud is sorted and combined with the point cloud position to form a coating path file for the free-form surface.

III. PLANE STACKING PRINTING

At present, the common path planning in 3D printing is Z-shaped, spiral, contour, and hybrid. The Z-shaped path is the

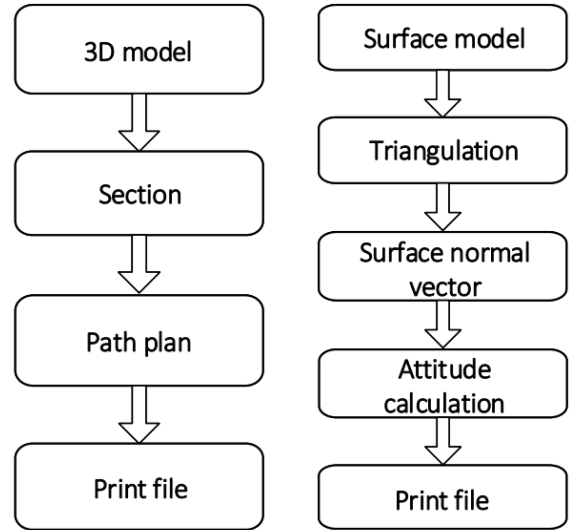


Fig. 2. Data processing flow for additive forming and free-form surface coating

most widely used and most commonly used. The spiral path is often used for high edge accuracy requirement. Occasionally, the contour line path is suitable for ring objects such as cups. They are shown in Fig. 3.

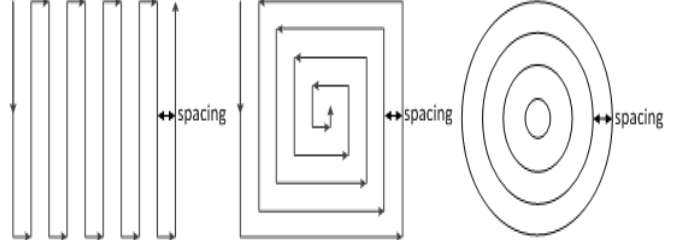


Fig. 3. Path diagram

For additive forming printing in plane, UR3 is not difficult to implement. Simply convert the planned path point to the world coordinates of UR3, and fix the nozzle attitude, set the speed and acceleration, then control UR3 with MoveL command to implement printing.

In the actual printing test, when UR3 has a fast moving speed, the actual path of the linear motion is not a straight line, but a random curve similar to a sine wave, so that the printing precision is low. UR3 controls its travel path by position, and cannot move the position when it does not reach the designated position, so the error cannot be eliminated.

In order to optimize the plane uniformity of printing, UR3 is controlled to move in a hybrid path, as shown in Fig. 4.

IV. FREE-FORM SURFACE COATING

The position and attitude control of the arm is the core technology for 3D printing. This paper introduces the calculation

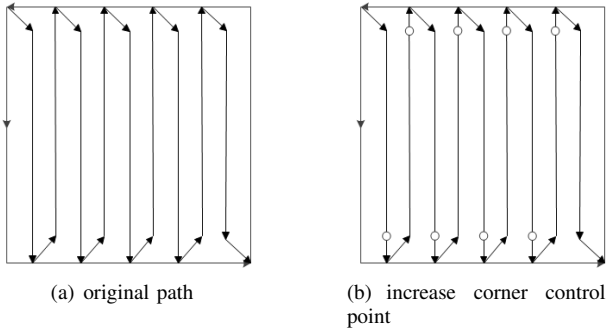


Fig. 4. Schematic diagram of the hybrid print path

method of the control parameters of UR3 for the free-form surface coating. For any free-form surface, the point cloud data on the surface is first obtained by a line laser scanner, and the path points with different intervals are restructured according to the printing requirements; then triangulation is performed, and the vertex normal vector of each triangle is calculated. Next, the attitude control parameters of UR3 are calculated based on the normal vector, and the final control vector is generated by combining the position parameters.

The surface model of Fig. 5 (a) is used to illustrate the data processing before using UR3 for the free-form surface spraying. The point cloud scanned by the line laser sensor is shown in Fig. 5 (b). It can be seen that the scanned point cloud has faults in the height direction, which have a great influence on the calculation of the normal vector of the point clouds and the accuracy of the final surface coating, so it is necessary to restructure the surface point cloud.

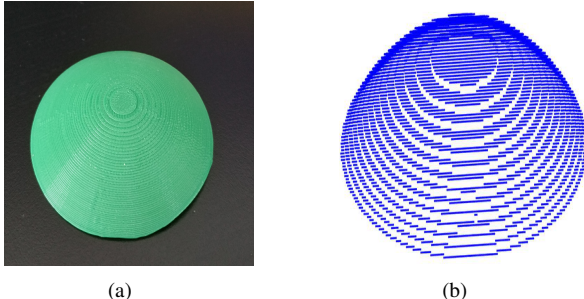


Fig. 5. Free-form surface model and point cloud

Considering the printing spacing, accuracy and convenience for subsequent calculation, the sensor scanning spacing of X-axis and Y-axis is 0.3mm and 1mm respectively. And in order to simplify the reconstruction algorithm, we use 2D point fitting instead of 3D surface reconstruction. Firstly, the cross section of X-axis of point cloud model is fitted, and then the cross section of Y-axis is fitted. The fitting method is the least squares method. Each set of points is fitted and then combined into a new 3D model. When the surface of the model is complex, the fitting function of each set of points can be different. This way ensures that the final generated surface model has higher precision. Take a set of points as an example

to illustrate, the results of the 6-time function fitting are closest to the original model, as shown in the Fig. 6 (a), indigo * indicates the origin cloud, blue points indicate the fitting result of four-power function, and red o points indicate the fitting result of six-power function. The original point cloud model and the fitted point cloud model are shown in Fig. 6 (b). The step effect error is eliminated after fitting.

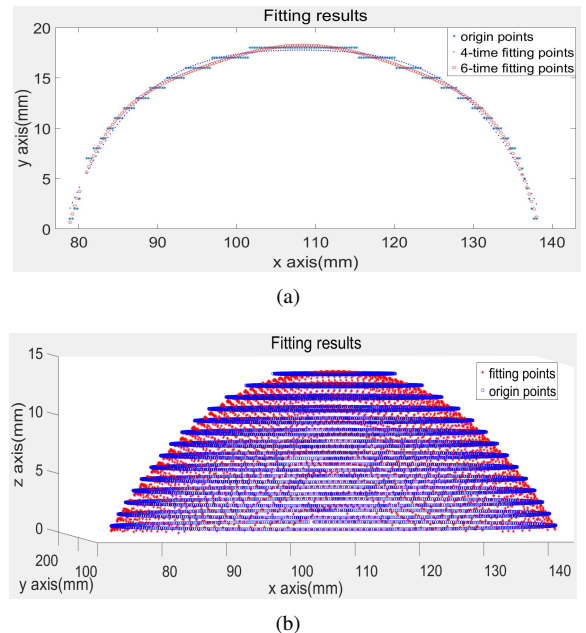


Fig. 6. Cross-section and overall point cloud fitting results

Next, the normal vector of each point in the point cloud model needs to be calculated as the attitude control parameter when UR3 is coating to the point. The triangulation is used for mesh processing, and the vectors are computed at vertices with respect to the neighbor cells. The calculation results are shown in the Fig. 7.

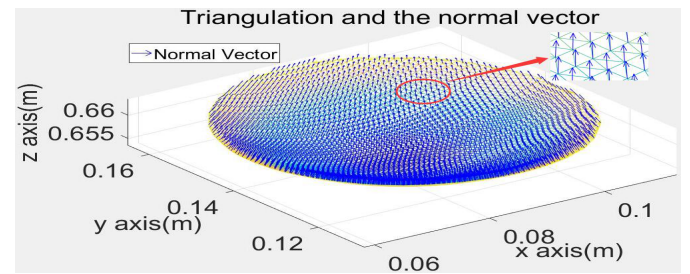


Fig. 7. Point cloud triangulation and normal vector calculation results

After obtaining the normal vector of each point, the attitude parameters of UR3 can be calculated. First calculates the corresponding Euler angle (roll, pitch, yaw) according to the normal vector, and then converts it into the rotation vector Rx, Ry, Rz which controls the attitude of UR3. Finally the 6-dimensional control vectors (x, y, z, Rx, Ry, Rz) of UR3 can be obtained by combining the position parameters x, y, z of the path points. The flow is shown in Fig. 8.

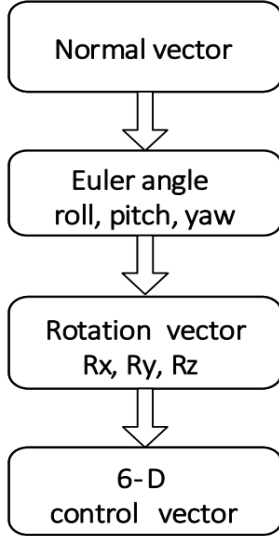


Fig. 8. Control vector calculation flow of UR3

Taking space vector [1 2 3] as an example, the calculation process of attitude parameters is illustrated, as shown in Fig. 9. When the attitude parameter is [0 0 0], the attitude of UR3 is as vector [0 0 1]. According to the definition of Euler angle, roll angle of vector [1 2 3] is 0.588 between vector [0 2 3] and vector [0 0 1] (expressed in radian), and the direction is negative; pitch angle is 0.322 between vector [1 0 3] and vector [0 0 1], and the direction is positive; yaw angle is 0.

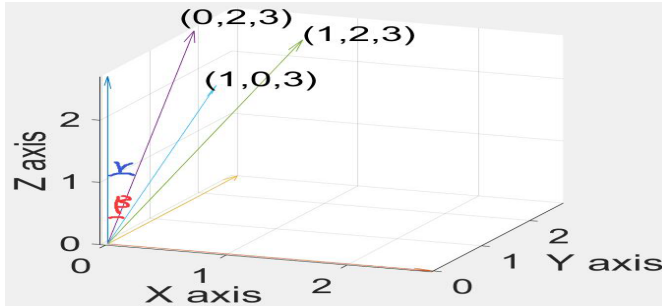


Fig. 9. Diagram of Euler angle calculation

For UR3, as the Euler angle is known, the rotation matrix is:

$$\begin{aligned}
 {}^bR(\gamma, \beta, \alpha) &= R_z(\alpha)R_y(\beta)R_x(\gamma) \\
 &= \begin{bmatrix} \cos\alpha & -\sin\alpha & 0 \\ \sin\alpha & \cos\alpha & 0 \\ 0 & 0 & 1 \end{bmatrix} \begin{bmatrix} \cos\beta & 0 & \sin\beta \\ 0 & 1 & 0 \\ -\sin\beta & 0 & \cos\beta \end{bmatrix} \begin{bmatrix} 1 & 0 & 0 \\ 0 & \cos\gamma & -\sin\gamma \\ 0 & \sin\gamma & \cos\gamma \end{bmatrix} \quad (1) \\
 &= \begin{bmatrix} r_{11} & r_{12} & r_{13} \\ r_{21} & r_{22} & r_{23} \\ r_{31} & r_{32} & r_{33} \end{bmatrix}
 \end{aligned}$$

Calculate the angle θ and k_x, k_y, k_z according to the rotation

matrix:

$$\begin{aligned}
 \cos\theta &= 2\cos^2\frac{\theta}{2} - 1 = 2\left(\frac{1}{2}\sqrt{1+r_{11}+r_{22}+r_{33}}\right)^2 - 1 \\
 &= \frac{r_{11}+r_{22}+r_{33}-1}{2} \\
 \theta &= \arccos\frac{r_{11}+r_{22}+r_{33}-1}{2} \\
 k_x &= \frac{r_{32}-r_{23}}{2\sin\theta} \\
 k_y &= \frac{r_{13}-r_{31}}{2\sin\theta} \\
 k_z &= \frac{r_{21}-r_{12}}{2\sin\theta}
 \end{aligned} \quad (2)$$

Then its rotation vector is:

$$[R_x \ R_y \ R_z]^T = [k_x\theta \ k_y\theta \ k_z\theta]^T \quad (3)$$

For vector [1 2 3], its $\gamma = 0.588$, $\beta = 0.322$, $\alpha = 0$, then its rotation vector is:

$$[R_x \ R_y \ R_z]^T = [-0.5829 \ 0.3124 \ 0.0946]^T \quad (4)$$

According to the calculation process above, 6-dimensional vectors of all path points of the free-form surface can be obtained, which is the path control file of UR3.

V. EXPERIMENT

UR3 can realize offline remote programming control through its own API library file, including C#, Python and so on. In order to facilitate the test of the path planning algorithm, UR3 control software was developed in the C# language on the VS platform, and the print control was implemented by reading the path file.

Before printing, the coordinates of the manipulator and the printing platform need to be calibrated, and the XY axis plane of the manipulator should be parallel to the platform. Set the planar print path as the Fig. 4, the print sample is shown in Fig. 10. When the moving speed of UR3 is fast and without pressure control, the printing path is not a straight line and the printing effect is bad, as shown in Fig. 10 (a); When the moving speed is 1mm/s, the printing path is straight, but there is material accumulation at the corners of the edge, as shown in Fig. 10 (b); After adding pressure control at the corner, the printing effect is as shown in Fig. 10 (c).

The free-surface coating experiment was carried out with the model of Fig. 5. The coating effect is shown in Fig. 11 by using Z-shaped path. From the results, we can see that the manipulator achieves the desired printing effect, but the printing accuracy still needs to be improved. When UR3 is used to carry out surface coatings, there will still be jitter at the moving speed of 1mm/s, while planar printing will not. Besides, the bigger the deflection angle of the end of UR3 is, the stronger the jitter is, which is a major factor affecting the printing accuracy. Another important factor affecting the printing accuracy is the extrusion speed of the material. When the extrusion speed is small, the straightness of the printing is good, but the material is likely to accumulate in the needle, which causes the material to be uneven during the coating. As shown in Fig. 11 (a); when the material extrusion speed

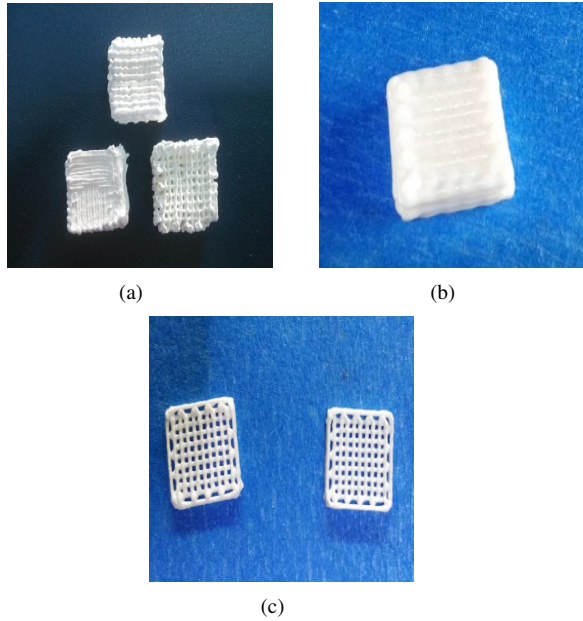


Fig. 10. Planar printing sample

is too fast, the printed material will appear jagged rather than straight, and the edges will also accumulate, as shown in Fig. 11 (b); It is necessary to find the corresponding relationship between the movement speed of the manipulator and the extrusion speed of the material through experiments to ensure the printing accuracy, as shown in Fig. 11 (c) is a better coating effect.

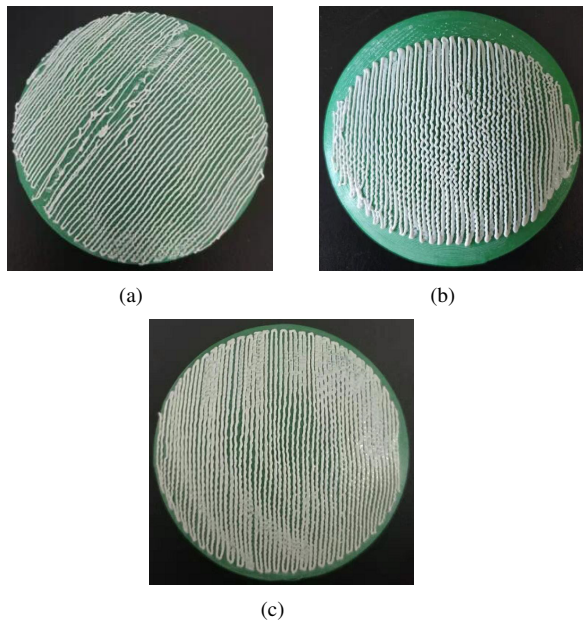


Fig. 11. Free-form surface coating effect

The third important factor affecting the printing accuracy is the fitting accuracy of the model surface. The closer the point cloud is to the original model, the higher the accuracy is. The fitting accuracy can be optimized by changing the fitting

parameters. Fig. 12 shows the fitting results and coating effect of another model.

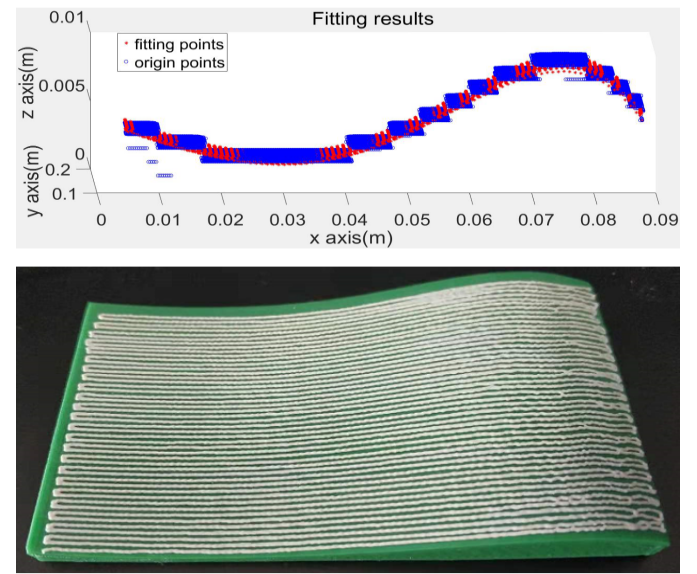


Fig. 12. Fitting results and coating effect

VI. CONCLUSION

In this paper, we introduce a comprehensive methodology to realize 3D printing of biomaterials by utilizing UR3 manipulators, especially the surface coating of the free-form surface models. The control algorithm of the manipulator is optimized through repeated experiments. And, the free-form surface reconstruction method proposed in this paper is simple and operable, which provides great convenience for the subsequent path planning of the manipulator. With a further insight, the overall process presented in this paper can also be applied in other applications such as spraying and provide a comprehensive reference for the robots which require high DOF operations.

ACKNOWLEDGMENT

This work was supported by the National Key Research and Development Program of China (No. 2016YFC11000501) and Laboratory of Robotics and Intelligent Systems (CAS, Quanzhou).

REFERENCES

- [1] Wallin T J , Pikul J , Shepherd R F . 3D printing of soft robotic systems[J]. Nature Reviews Materials, 2018
- [2] Ngo T D , Kashani A , Imbalzano G , et al. Additive manufacturing (3D printing): A review of materials, methods, applications and challenges[J]. Composites Part B Engineering, 2018, 143
- [3] Jammalamadaka U , Tappa K. Recent advances in biomaterials for 3D printing and tissue engineering[J]. Journal of functional biomaterials, 2018, 9(1): 22
- [4] Lipskas J , Deep K , Yao W. Robotic-assisted 3D bio-printing for repairing bone and cartilage defects through a minimally invasive approach[J]. Scientific reports, 2019, 9(1): 3746
- [5] Wang X , Jiang M , Zhou Z , et al. 3D printing of polymer matrix composites: A review and prospective[J]. Composites Part B Engineering, 2017, 110:442-458.

- [6] Laronda M M , Rutz A L , Xiao S , et al. A bioprosthetic ovary created using 3D printed microporous scaffolds restores ovarian function in sterilized mice[J]. *Nature Communications*, 2017, 8:15261
- [7] Wang X , Rijff B L , Khang G . A buildingblock approach to 3D printing a multichannel, organregenerative scaffold[J]. *Journal of Tissue Engineering & Regenerative Medicine*, 2015, 11(5):1403
- [8] Lee V , Singh G , Trasatti J P , et al. Design and Fabrication of Human Skin by Three-Dimensional Bioprinting[J]. *Tissue Engineering Part C: Methods*, 2014, 20(6):473-484
- [9] Mu Suyi. The Research of the generation of the spraying robot trajectory based on the point cloud slicing[D]. Jiangsu University, 2009
- [10] Li M Z , Lu Z P , Sha C F , et al. Trajectory Generation of Spray Painting Robot Using Point Cloud Slicing[J]. *Applied Mechanics and Materials*, 2010, 44-47:1290-1294
- [11] Zheng H , Cong M , Liu D , et al. Automatic path and trajectory planning for laser cladding robot based on CAD[C]// 2016 IEEE International Conference on Mechatronics and Automation. IEEE, 2016
- [12] Chen S , Wu C , Shuai X , et al. Fast registration of 3D point clouds with offset surfaces in precision grinding of free-form surfaces[J]. *International Journal of Advanced Manufacturing Technology*, 2018(17):1-12
- [13] Wang G , Cheng J , Li R , et al. A new point cloud slicing based path planning algorithm for robotic spray painting[C]// 2015 IEEE International Conference on Robotics and Biomimetics (ROBIO). IEEE, 2015
- [14] Kim C , Espalin D , Cuaron A , et al. Cooperative Tool Path Planning for Wire Embedding on Additively Manufactured Curved Surfaces Using Robot Kinematics[J]. *Journal of Mechanisms and Robotics*, 2015, 7(2):021003
- [15] Wang Z , Liu R , Sparks T , et al. Realisation of robot ink deposition on a curved surface[J]. *International Journal of Computer Applications in Technology*, 2016, 53(2):183
- [16] Barnett E , Gosselin, Clment. Large-Scale 3D Printing With A Cable-Suspended Robot[J]. *Additive Manufacturing*, 2015, 7:27-44
- [17] Chengkai D , Wang C C L , Chenming W , et al. Support-free volume printing by multi-axis motion[J]. *ACM Transactions on Graphics*, 2018, 37(4):1-14